Geophysical Research Letters

RESEARCH LETTER
10.1029/2018GL081211

Remarkable Control of Western Boundary Currents by *Eddy Killing*, a Mechanical Air-Sea Coupling Process

L. Renault[1,2], P. Marchesiello[2], S. Masson[3], and J. C. McWilliams[2]

[1]LEGOS, University of Toulouse, IRD, CNRS, CNES, UPS, Toulouse, France, [2]Atmospheric and Oceanic Sciences, University Of California, Los Angeles, CA, USA, [3]Sorbonne Universités (UPMC, Univ Paris 06)-CNRS-IRD-MNHN, LOCEAN Laboratory, Paris, France

Key Points:
- The oceanic inverse energy cascade is weakened by *eddy killing* associated with current feedback during eddy-wind interaction
- Western boundary currents are subdued by *eddy killing* through weakened inverse energy cascade
- The spectral energy flux is validated using satellite currents; these data underestimate eddy-mean flow interaction due to coarse resolution

Correspondence to:
L. Renault,
lionel.renault@ird.fr

Citation:
Renault, L., Marchesiello, P., Masson, S., & McWilliams, J. C. (2019). Remarkable control of western boundary currents by eddy killing, a mechanical air-sea coupling process. *Geophysical Research Letters*, *46*, 2743–2751. https://doi.org/10.1029/2018GL081211

Received 6 NOV 2018
Accepted 27 FEB 2019
Accepted article online 4 MAR 2019
Published online 14 MAR 2019

Abstract Western boundary currents (WBCs) are critical to Earth's climate. In the last decade, mesoscale air-sea interactions emerged as an important factor of WBC dynamics. Recently, coupled models including the feedback of surface oceanic currents to the atmosphere confirmed the existence of a physical process called eddy killing, which may correct long-lasting biases in the representation of WBCs by providing an unambiguous energy sink mechanism. Using ocean-atmosphere coupled simulations of the Gulf Stream and the Agulhas Current, we show that eddy killing reduces the eddy-mean flow interaction (both forward and inverse cascades) and leads to more realistic solutions. Model and data fluxes are in good agreement when the same coarse grid is used for their computation, although in this case they are underestimated. We conclude that the uncoupled approach is no longer suitable for continued ocean model improvement and discuss new formulations that should better account for air-sea interactions.

Plain Language Summary Western boundary currents (WBCs), such as the Gulf Stream and the Agulhas Current play a crucial role in global ocean circulation and in determining and stabilizing the Earth's climate. In the last decade, mesoscale air-sea interactions emerged as important in WBC dynamics. Recently, coupled models including the feedback of surface oceanic currents to the atmosphere revealed a process called eddy killing, which potentially corrects long-lasting biases in the representation of WBCs. In this study, using ocean-atmosphere coupled simulations of the Gulf Stream and Agulhas Current, we show that eddy killing reduces the interactions between eddies and mean flow. The influence of the eddies on the mean flow can be measured by the cascade of energy, and, in particular, the inverse cascade of energy. The reduction of inverse energy flux by eddy killing leads to realistic solutions and, in particular, to the observed stabilization of WBCs. Model and data fluxes are in good agreement when the same coarse grid is used for their computation, although in this case they are underestimated. We conclude that uncoupled models are no longer suitable for continuing our model improvement of ocean dynamics and discuss new formulations that should better account for air-sea interactions.

1. Introduction

Western boundary currents (WBCs)—Gulf Stream (GS), Kuroshio, Agulhas Current (AC), East Australia, Somalia Current, and Brazil Currents—are the strongest oceanic currents on Earth and major features of the global ocean circulation that largely controls the Earth's climate. Understanding their equilibrium, variability, and trend is critical to oceanic and climate research.

There are still major gaps in our knowledge of ocean dynamics, despite numerous international programs of observation and modeling. The separation of WBCs was associated early on with coastal curvature and the inertia needed to overcome topographic steering, with some control (for the GS) from counterflowing deep WBCs (Spall, 1996). More recently, emblematic features of WBCs appeared tied in ocean models to the resolution of mesoscale activity through eddy-mean flow interaction (McWilliams, 2008) and a spatial resolution of 1/10° was suggested as a minimum for properly representing the GS separation (Bryan et al., 2007; Chassignet & Marshall, 2008). Therefore, large improvements were expected from the increase of computing power and grid resolution. If this was verified to an extent, the simulated eddy energy has now become excessive in WBCs. Specifically, according to Özgökmen and Chassignet (2002), an excess of mesoscale activity at the separation point leads to unrealistic WBC separation from the coastline. An energy sink is thus needed in high-resolution, mesoscale resolving models. This can be provided by dissipation terms used as

turbulence closure models (e.g., Bryan et al., 1995, 2007; Chassignet & Marshall, 2008; Chassignet & Xu, 2017). However, this approach disagrees with quasi-geostrophic theory that predicts an inverse cascade of energy toward larger scales. A direct energy transfer toward dissipation is still possible due to loss of balance at submesoscale (see Gula et al., 2016 for the GS), but theoretically limited.

In parallel to improved resolution and more accurate numerical techniques, supercomputers also favored the emergence of regional coupled models, and a growing interest in fine-scale air-sea interactions. At first, attention was essentially given to the feedback of sea surface temperature (SST) on the air flow (e.g., Chelton et al., 2004; Ma et al., 2016; Minobe et al., 2008). Progressively, the issue of stress interaction has emerged, that is, the feedback effect of surface currents on the stress and overlying winds (process called *current feedback* or *top drag*; see Bye, 1985; Dewar & Flierl, 1987; Duhaut & Straub, 2006; Eden & Dietze, 2009; Luo et al., 2005; McClean et al., 2011; Renault, Molemaker, Mcwilliams, et al., 2016). Quite unexpectedly, the latter happens to correct some long-standing modeling biases in eddy-mean flow interaction, providing an undeniable energy sink mechanism with no need for large internal dissipation.

There are two main effects of current feedback on the ocean circulation: a large-scale and a mesoscale effect. At the larger scales neglecting current feedback leads to an overestimation of wind work, leading to overly strong currents (Luo et al., 2005; Pacanowski, 1987; Renault, Molemaker, Gula, et al., 2016, Renault, McWilliams, Penven, et al., 2017; Scott & Xu, 2009). The local effect is less intuitive. It was first suggested by Bye (1985) but largely ignored, then confirmed more recently by the advent of eddy-rich coupled models. This eddy-wind interaction process consists of a drastic reduction by roughly 30% of oceanic mesoscale and submesoscale activity (Seo et al., 2015; Renault, Molemaker, Mcwilliams, et al., 2016, Renault, Molemaker, Gula, et al., 2016, Renault, McWilliams, Penven, et al., 2017, 2018; Seo, 2017; Oerder et al., 2018). This dampening effect, called *eddy killing*, is caused by a negative eddy wind work, that is, a sink of energy from mesoscale currents to the atmosphere (Renault, Molemaker, Mcwilliams, et al., 2016, Renault, McWilliams, Masson, et al., 2017; Scott & Xu, 2009; Xu & Scott, 2008). Renault, Molemaker, Gula, et al. (2016) and Renault, McWilliams, and Penven (2017) show that in numerical models eddy killing improves the representation of the GS path and the location of AC retroflection where the current returns eastward to the South Indian Ocean.

In this study, a set of eddy-rich ocean-atmosphere coupled simulations, with or without including current feedback (CFB or NOCFB simulations) are carried out over the North Atlantic Basin and the Greater Agulhas regions for the period 2000–2005. Our main objective is to extend the results of Renault, Molemaker, Gula, et al. (2016) and Renault, McWilliams, and Penven (2017) by investigating the control mechanisms by which eddy killing affects WBCs and to quantify oceanic eddy-mean energy transfers.

2. Model, Data, and Methods

The numerical models and configurations used in this study are presented in Renault, Molemaker, Gula, et al. (2016) and Renault, McWilliams, and Penven (2017). The material in this section comes from these references, with minor variations.

2.1. The CROCO Model

The oceanic simulations were performed with the Coastal and Regional Ocean Community Model (CROCO; Debreu et al., 2012), developed around the kernel of the Regional Oceanic Modeling System (Shchepetkin & McWilliams, 2005). CROCO is a free-surface, terrain-following coordinate model with split-explicit time stepping and with Boussinesq and hydrostatic approximations (in this application). The North Atlantic grid covers the North Atlantic subtropical and subpolar gyres, extending from 133.7°W to 21.7°W and from 0.4°N to 73.2°N; its grid size is 1,152 × 1,059 points and grid resolution 6–7 km. The Greater Agulhas grid covers the South African region, including the Mozambique Channel, Madagascar, AC retroflection, and Benguela upwelling system, extending from 11.5°W to 50.0°E and from 44.4°S to 5.0°S; its grid size is 1,031 × 749 points and grid resolution between 4.5 and 6 km (4.8 km over the Agulhas Basin region). Both simulations have 50 vertical levels; the vertical grid is stretched for increased resolution in the boundary layers, using stretching surface and bottom parameters $\theta_s = 7$ and $\theta_b = 2$; high resolution in the thermocline is also provided with stretching parameter $h_{\text{cline}} = 300$ m.

The model is initialized using January climatology from the Simple Ocean Data Assimilation (Carton & Giese, 2008) and is spun up for 5.5 years using seasonal atmospheric surface fluxes and oceanic boundary

conditions, until the model reaches an equilibrium state. It is then run for an additional period, from June 1999 to 2004, using interannual surface fluxes and oceanic forcing from monthly Simple Ocean Data Assimilation analyses, introduced through mixed active-passive open boundary conditions (Marchesiello et al., 2001). Vertical mixing of tracers and momentum is given by the K-profile parameterization (Large et al., 1994), and the diffusive part of the lateral advection scheme for tracers is rotated along isopycnal surfaces to avoid spurious diapycnal mixing (Lemarié et al., 2012; Marchesiello et al., 2009).

2.2. The WRF model

For both domains, as in Renault, Molemaker, Gula, et al. (2016) and Renault, McWilliams, and Penven (2017), Weather Research and Forecast (WRF) model (Skamarock et al., 2008), version 3.7.1, is implemented in a single-grid configuration. It is run as a regional downscaling of the Climate Forecast System Reanalysis (Saha et al., 2010). Climate Forecast System Reanalysis is available with a resolution of about 40 km and is used for initialization on 1 June 1999 and boundary forcing for 5.5 years. WRF computational domain encompasses that of the ocean model domain to avoid the effect of WRF sponges (four-point wide) with horizontal resolution of about 18 km. For parameterizations (boundary layer, convection, microphysics, radiation, etc.), the reader is referred to Renault, McWilliams, and Penven (2017). More importantly here, a bulk formula (Fairall et al., 2003) is used in the boundary layer model to estimate the surface turbulent freshwater and momentum fluxes, which are subsequently provided to CROCO.

2.3. Coupling Experiments

The OASIS3 coupler is used to exchange data fields every hour between CROCO and WRF (Valcke, 2013). In this study, we consider some of the experiments described in Renault, Molemaker, Gula, et al. (2016) and Renault, McWilliams, and Penven (2017). For both the North Atlantic and Greater Agulhas domains, we use two experiments: in the first one (called NOCFB for no current feedback) WRF forces CROCO every hour with hourly averages of freshwater, heat, and momentum fluxes; at the end of each cycle CROCO provides WRF with an updated hourly (mean) SST. The surface stress is estimated using the absolute wind U_a (computed at the first vertical level in WRF). The second experiment with current feedback (CFB) is similar, but this time CROCO provides WRF not only with SST but also with the updated surface current $\boldsymbol{U_o}$ (computed at the upper vertical level in CROCO). In this case, the surface stress is estimated from the wind U relative to the moving ocean surface:

$$\boldsymbol{U = U_a - U_o} \tag{1}$$

2.4. AVISO Altimetry

Daily absolute dynamic topography fields are obtained from the Archiving, Validation, and Interpretation of Satellite Oceanographic data (AVISO) product (Ducet et al., 2000). Maps of sea level anomaly are constructed on a grid of 0.25° resolution by space-time optimal interpolation from combined and intercalibrated altimeter missions (Le Traon et al., 1998). Then, absolute dynamic topography is produced by adding to the sea level anomaly a mean dynamic topography computed from a combination of oceanic observations and an ocean general circulation model solution (Rio et al., 2014).

3. Results

The sink of mesoscale energy to the atmosphere is naturally ignored in uncoupled WBC model simulations. These simulations suffer from two enduring biases concerning WBC patterns: AC retroflection and GS separation and penetration into the North Atlantic basin (Loveday et al., 2014; Schoonover et al., 2016; Renault, Molemaker, Gula, et al., 2016; Renault, McWilliams, Penven, et al., 2017). Eddy killing was shown to control essential characteristics of these features, partially correcting model biases. Figures 1a–1c illustrate the GS case. From satellite observation, the GS presents a unique, very stable mode of separation at Cape Hatteras and a straight eastward penetration into the interior of the Atlantic Basin. By contrast, an excessive number of eddies are generated in the NOCFB simulation without eddy killing effect, then detach from the current path and interact with it, causing excessive GS meandering. Eddies can propagate back to the coast where they interfere with the mean flow, causing a bimodal GS separation. With eddy killing (CFB simulation), eddy activity and lifetime are reduced by ~30%, which brings it to more realistic levels (Renault, McWilliams, Penven, et al., 2017). Eddies have less interaction with the mean flow and fewer propagate back to the coast. Concurrently, GS separation and penetration is more stable and very similar to observations.

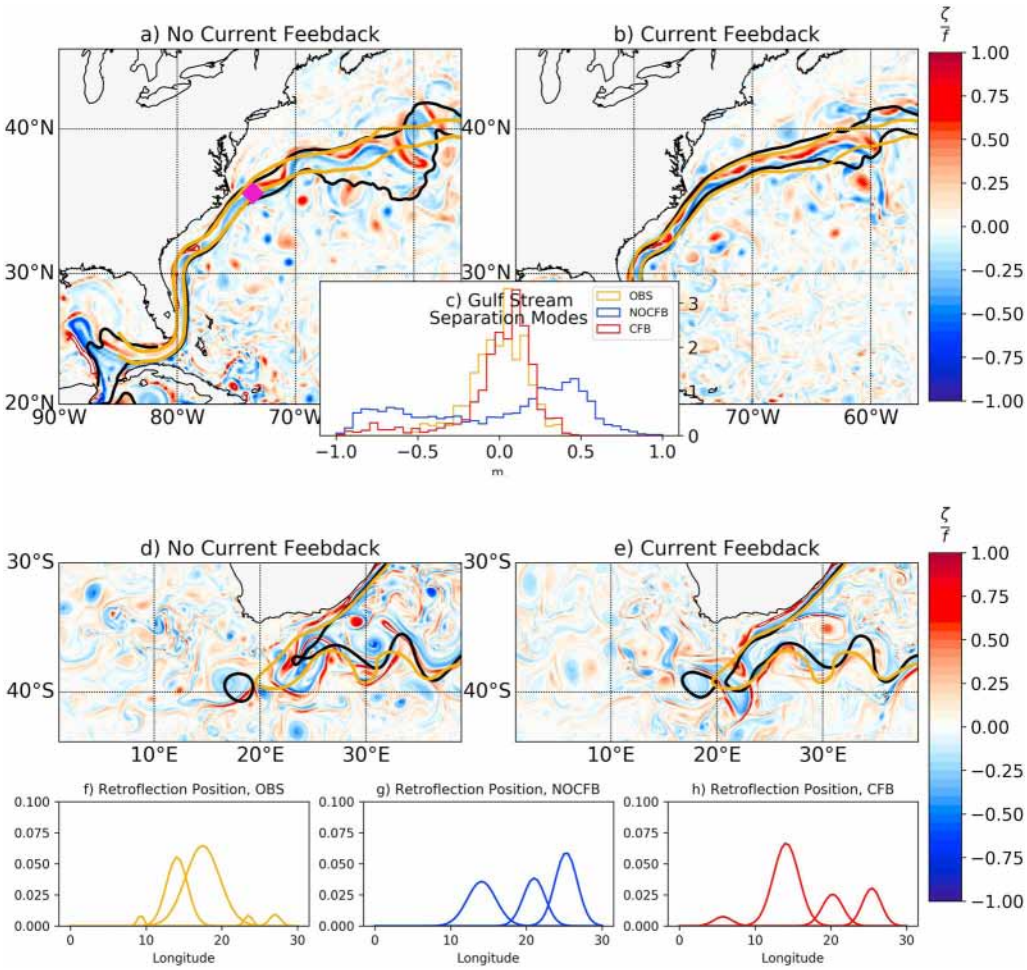

Figure 1. *Eddy killing* improves the Gulf Stream (GS) and Agulhas Current (AC) retroflection position in simulations. The color field presents a typical snapshot of surface relative vorticity ($\frac{\zeta}{f}$) from (a, d) coupled simulations without current feedback to the wind (NOCFB) and (b,e) coupled simulations with current feedback (CFB). Black contour lines represent the simulated long-term mean GS path (contour of 0.6 m/s and mean AC retroflection (contour of 0.35 m). The yellow contour lines shows the observed GS path (contour of 0.6 m/s) and AC retroflection (contour of 0.35 m). (c) Probability density function of sea level anomaly around the diamond box (indicated in panel a) from AVISO (yellow), NOCFB (blue), and CFB (red). (f) Modes of the AC retroflection zonal position as estimated by Renault, McWilliams, and Penven (2017) and represented by the Gaussian fits of the significant Zonal probability density function peaks of the AC retroflection location from AVISO (2000–2004), (g) NOCFB, and (h) CFB. The eddy-resolving coupled model with CFB rectifies long-standing biases in oceanic models of bimodal and unsteady GS separation and for the AC, overrepresentation of its upstream mode of retroflection. AVISO = Archiving, Validation, and Interpretation of Satellite Oceanographic.

Similar positive results are found for the AC retroflection (Figures 1d–1h). Here as well, eddy-wind interaction induces a large sink of energy from the mesoscale currents to the atmosphere, reducing mesoscale activity by ~27% (Renault, McWilliams, Penven, et al., 2017). Satellite detection of mean sea surface height is a good indicator of the mean longitudinal position of AC retroflection, which is around 18°E (Figures 1d and 1e; Loveday et al., 2014). The position of AC retroflection is usually stable, although at times it shifts upstream to the east. A simulation without current feedback overestimates the frequency of upstream retroflection (Figure 1g), resulting in a mean position located too far east. Eddy killing significantly reduces this bias (Figure 1h), shifting the distribution of locations to the west in better agreement with observations.

In the ocean, mesoscale energy feeds back to the large-scale circulation through eddy-mean flow interaction—the inverse energy cascade (e.g., Arbic et al., 2013; Capet et al., 2008; LaCasce, 2012). Because mesoscale eddies compose a huge reservoir of oceanic energy, the inverse cascade operates a tight control on the general circulation. Stabilization of the GS and improvement of the AC retroflection may be explained

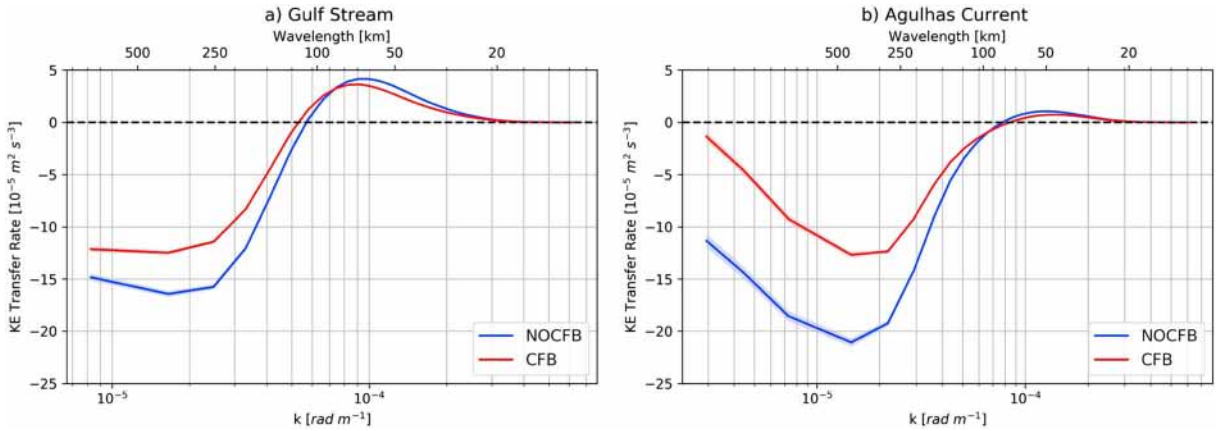

Figure 2. Spectral flux $\pi_{KE}(k)$ of surface oceanic geostrophic kinetic energy in (a) the Gulf Stream and (b) the Agulhas Current, for coupled simulations with current feedback (CFB, red) and without current feedback (NOCFB, blue). The shaded curves represent the associated error as estimated using a bootstrap method. *Eddy killing* induces a large reduction of the inverse energy cascade, responsible for Gulf Stream stabilization and for the observed Agulhas retroflection position.

by a reduction of the inverse energy cascade, as we now show. As in Marchesiello et al. (2011) and Arbic et al. (2013), the spectral kinetic energy flux $\Pi(k)$, that is, the energy transfer rate in k space, is computed from the surface geostrophic flow obtained from the coupled simulations and from AVISO gridded altimeter data (Ducet et al., 2000). Specifically, $\Pi(k)$ is the integral in k of the KE advection term $A(k)$, assuming that the flux vanishes at the highest wavenumber $k_{\max}$. $A(k)$ is given by

$$A(k) = A_H(k) + A_V(k) = \Re\left[\overline{-\widehat{\mathbf{u}_h^*} \cdot (\widehat{\mathbf{u}_h \cdot \nabla)\mathbf{u}_h} - \widehat{\mathbf{u}_h^*} \cdot \widehat{w\frac{\partial \mathbf{u}_h}{\partial z}}}\right] \tag{2}$$

where the caret denotes a horizontal Fourier transform after removing the areal mean and performing symmetrization, to avoid edge effects in the periodization process. The asterisk notation * indicates the complex conjugate operator; the symbol $\Re$ represents the real part operator; the overbar represents an average in time over the whole period of the simulation (5 years). Then $\Pi(k)$ is computed as

$$\Pi(k) = \int_k^{k_{\max}} A \quad \mathrm{d}k \tag{3}$$

The error associated with the computation of $\Pi(k)$ is assessed using a bootstrap method; $\Pi(k)$ is computed 10,000 times using random samples from the distribution. The error bars are defined as plus or minus the standard deviation of the obtained $\Pi(k)$. Fluxes for the GS are assessed over the subregion: [76.2–38°W; 31.8°N 41.7°N] and for the AC over the subregion:[2.5°W to 48°E; 43.2°S 37.6°S] (Figure 2). From a wavelength of about 100 km, both forward and inverse energy transfers are identified by positive and negative lobes, respectively. Following, for example, Arbic et al. (2013), the relative size of the forward and inverse cascades is measured by F/I defined as follows:

$$F/I = -\frac{\text{maximum positive value of } \Pi(k) \text{ at small scales}}{\text{minimum negative value of } \Pi(k) \text{ at large scales}} \tag{4}$$

A small value of F/I indicates an inverse cascade larger than the forward cascade. In the simulations without current feedback, $F/I = 0.26$ and 0.05 for the GS and AC, respectively (Figure 2). Both WBCs are characterized by an inverse energy cascade much larger than the forward energy cascade starting at the injection scale. Therefore, most of the large reservoir of mesoscale energy injected by baroclinic and barotropic instabilities feeds back to large scale currents, while a smaller part is lost to small dissipative scales. This is the tight control exerted by eddies on WBCs (McWilliams, 2008). Eddy killing, by damping mesoscale activity, has an indirect effect on energy pathways: it somewhat reduces the forward cascade by 12% and 25% over GS and AC, respectively; but more importantly here, it largely reduces the inverse energy cascade (by 30% and 43%, respectively). As a result, F/I slightly increases from 0.26 to 0.29 for GS and from 0.05 to 0.06 for AC. In coupled simulations without current feedback (or fully uncoupled simulations), the sink of energy

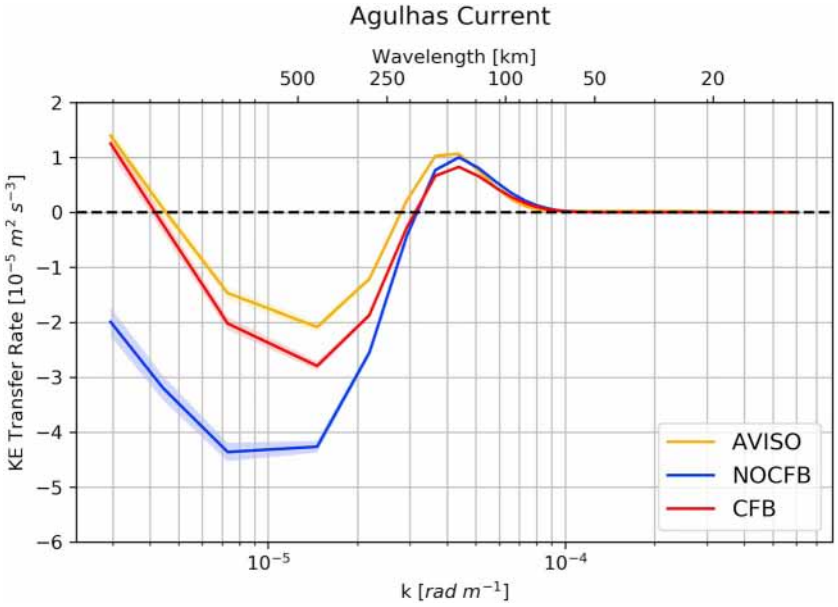

Figure 3. Spectral flux $\pi_{KE}(k)$ of surface ocean geostrophic kinetic energy over the Agulhas Current (same box as Figure 2) from AVISO (yellow), and *filtered* coupled simulations with current feedback (CFB, red) and without current feedback (NOCFB, blue; see text for more details). The shaded curves represent the associated error as estimated using a bootstrap method. Fully coupled simulations (CFB) have a more realistic energy flux $\pi_{KE}(k)$ with respect to AVISO. AVISO = Archiving, Validation, and Interpretation of Satellite Oceanographic.

from mesoscale eddies to the atmosphere is missing, resulting in excessive mesoscale energy that boosts the inverse energy transfer in both WBCs.

The spectral energy flux can also be computed from satellite sea surface height data, which provides a validation for our analysis of WBC dynamics. However, AVISO has a coarse spatial resolution and, due to the interpolation procedure, is only able to resolve eddies with radius longer than about 40 km and lifetime longer than a week (Chelton et al., 2011). Arbic et al. (2013) show that this limitation strongly affects the computation of $\Pi(k)$. Therefore, a fair model-data comparison requires smoothing the model solutions to the same level as the data. We use a 7-day time averaging and a spatial Gaussian filter with a cutoff of ~40 km. $\Pi(k)$ is computed from the filtered model solutions and compared with AVISO (Figure 3). Consistent with Arbic et al. (2013), the forward energy cascade is shifted to lower wavenumbers compared with fluxes computed from the original solution, and the negative lobe of $\Pi(k)$ at large scales is drastically weakened by ~75%. This is a clear indication that the inverse energy cascade estimated from AVISO data is largely underestimated. (We checked that the smoothing procedure used for the model solution does not affect the AVISO estimation when the same procedure is applied to this data.) Over the AC, the inverse cascade for the filtered CFB solution (fully coupled) is much closer to that of AVISO than the filtered NOCFB solution. F/I reaches values of 0.23, 0.40, and 0.66 for AVISO, filtered CFB and NOCFB solutions, respectively. Similar results are found for the GS (not shown). Therefore, when accounting for eddy killing and its associated sink of energy, coupled simulations show better agreement of energy fluxes with AVISO data.

4. Discussion

We conclude that a poor representation of GS separation/penetration and AC retroflection position in uncoupled models can be explained by the missing eddy killing process. Most research studies in the recent past have relied on dissipation processes to correct simulation biases, but only few improvements were reported on other missing dynamical processes. One relevant finding in the last two decades is the key role played by topographic steering in WBC dynamics (Couvelard et al., 2008; Gula et al., 2015), which goes far beyond the idealized representation of western boundaries as solid walls.

However, higher resolution and improved topographic treatment did not solve the energy budget issue because oceanic mesoscale energy was then produced in excess and requires an energy sink to stabilize and accurately position the mean current paths. In Chassignet and Xu (2017), a subgrid-scale eddy viscosity is

added to numerical hyperviscosity (used for selective damping of numerical dispersion generated by centered advection schemes, akin to the implicit diffusion part of the third-order upstream-biased advection scheme in CROCO; see Marchesiello et al., 2009). The added dissipation is rationalized by mesoscale damping processes that are not resolved by the model (Chassignet & Garraffo, 2001). It allows to produce a correct mean GS path with an uncoupled 1/50° resolution Hybrid Coordinate Ocean Model setup. However, even though the simulated mesoscale variability at the separation point (Cape Hatteras) compares favorably with AVISO data, there is still too large a spread of mesoscale activity after separation (Figure 14 in Chassignet & Xu, 2017), reflecting excessive meandering similar to our NOCFB simulation. The added dissipation helps but appears as an ad hoc fix for processes that are not represented in the model, such as eddy killing. The challenge here is to justify a forward route to dissipation when geostrophic turbulence is characterized by an inverse cascade. Looking into it with a submesoscale resolving model (200-m resolution), Gula et al. (2016) recently found that GS interaction with topography can generate submesoscale centrifugal instability and some amount of energy dissipation, but only near the continental slope. An interior route to dissipation associated with submesoscale instabilities at the ocean surface is also proposed (Capet et al., 2008; Molemaker et al., 2010) but cannot account for large offshore dissipation past the separation point, where even numerical dissipation needed to damp numerical dispersion errors appears to be in excess (Marchesiello et al., 2011; Soufflet et al., 2016). While the route to dissipation in the ocean is being debated, mesoscale air-sea coupling offers a unambiguous physical process for the required sink of energy to achieve proper equilibrium in WBC systems and elsewhere.

The role of fine-scale ocean-atmosphere coupling modifies the usual conception of wind-driven currents. The wind is not just a large-scale energy source that initiates a turbulent cascade; it also interacts at fine scale and directly affects the entire oceanic spectrum. High-resolution coupled models have thus become essential tools that are now more easily accessible—at least regional models. Alternatively, for uncoupled ocean models, new formalisms should be designed to account for atmospheric adjustments and provide accurate oceanic energy sink. A major step will then be expected in the representation of currents, water masses, overturning circulation, oceanic ventilation, carbon uptake, etc. In particular, the boosting effect of oceanic eddies on marine productivity in nutrient-poor regions should be revisited through the lenses of eddy-wind interaction, as initiated by McGillicuddy et al. (2007). Anticyclonic eddies could sustain primary production over long distances due to surface Ekman pumping induced by the same eddy-wind interaction that dampens the eddy energy. This effect is again missing in usual oceanic model simulations.

Overall, the results presented here call for a change of paradigm in our representation of the ocean interface. The uncoupled approach is no longer suitable for continued ocean model improvement, unless new formulations can be devised that better account for air-sea interactions. Those should replicate a partial re-energization of the ocean by winds that are modified by surface currents—avoiding redundant energy sink in uncoupled models if fully using equation (1). Different approaches are possible. One consists of correcting the relative wind using a current-wind coupling coefficient s_w defined by $U = U_{\boldsymbol{a}} - (1 - s_w)U_{\boldsymbol{o}}$ (Renault, Molemaker, Mcwilliams, et al., 2016), or the surface stress using a current-stress coupling coefficient s_τ defined by $\tau = \tau_{\boldsymbol{a}} + s_\tau U_{\boldsymbol{o}}$ (Renault, McWilliams, Masson, et al., 2017); s_w and s_τ can be estimated from a coupled simulation although s_τ can also be parameterized as a function of the large-scale wind. Yet another approach would be based on the coupling of a simple atmospheric boundary layer model (a *slab* model for the lower atmosphere; e.g., Lemarié et al., 2017), in place of a full atmospheric model. In all cases, the results should be compared with fully coupled simulations, specifically looking at the sink of energy from eddy-wind interaction, and more generally at mesoscale activity and large scale currents.

Acknowledgments
We appreciate support from the National Science Foundation (OCE-1419450). This work used GENCI computing resources and the Engineering Discovery Environment (XSEDE). Data can be downloaded from https://tinyurl.com/ycb7ob6k website. The authors thank Eric Chassignet and one anonymous reviewer for useful discussions.

References

Arbic, B. K., Polzin, K. L., Scott, R. B., Richman, J. G., & Shriver, J. F. (2013). On eddy viscosity, energy cascades, and the horizontal resolution of gridded satellite altimeter products. *Journal of Physical Oceanography*, *43*(2), 283–300.

Bryan, F. O., Böning, C. W., & Holland, W. R. (1995). On the midlatitude circulation in a high-resolution model of the North Atlantic. *Journal of Physical Oceanography*, *25*(3), 289–305.

Bryan, F. O., Hecht, M. W., & Smith, R. D. (2007). Resolution convergence and sensitivity studies with North Atlantic circulation models. Part I: The western boundary current system. *Ocean Modelling*, *16*(3), 141–159.

Bye, J. A. (1985). Large-scale momentum exchange in the coupled atmosphere-ocean. *Elsevier Oceanography Series*, *40*, 51–61.

Capet, X., McWilliams, J., Molemaker, M., & Shchepetkin, A. (2008). Mesoscale to submesoscale transition in the California Current System. Part I: Flow structure, eddy flux, and observational tests. *Journal of Physical Oceanography*, *38*, 29–43.

Carton, J. A., & Giese, B. S. (2008). A reanalysis of ocean climate using Simple Ocean Data Assimilation (SODA). *Monthly Weather Review*, *136*(8), 2999–3017.
Chassignet, E. P., & Garraffo, Z. D. (2001). Viscosity parameterization and the Gulf Stream separation. In *From Stirring to Mixing in a Stratified Ocean: Proc. 'Aha Huliko'a Hawaiian Winter Workshop* (pp. 39–43). Honolulu, HI: University of Hawaii at Manoa.
Chassignet, E. P., & Marshall, D. P. (2008). *Gulf Stream separation in numerical ocean models. Geophyscial Monograph Series* (Vol. 177, pp. 39–61).
Chassignet, E. P., & Xu, X. (2017). Impact of horizontal resolution (1/12 to 1/50) on Gulf Stream separation, penetration, and variability. *Journal of Physical Oceanography*, *47*(8), 1999–2021.
Chelton, D. B., Schlax, M. G., Freilich, M. H., & Milliff, R. F. (2004). Satellite measurements reveal persistent small-scale features in ocean winds. *science*, *303*(5660), 978–983.
Chelton, D. B., Schlax, M. G., & Samelson, R. M. (2011). Global observations of nonlinear mesoscale eddies. *Progress in Oceanography*, *91*(2), 167–216.
Couvelard, X., Marchesiello, P., Gourdeau, L., & Lefèvre, J. (2008). Barotropic zonal jets induced by islands in the southwest Pacific. *Journal of Physical Oceanography*, *38*(10), 2185–2204.
Debreu, L., Marchesiello, P., Penven, P., & Cambon, G. (2012). Two-way nesting in split-explicit ocean models: Algorithms, implementation and validation. *Ocean Modelling*, *49*, 1–21.
Dewar, W. K., & Flierl, G. R. (1987). Some effects of the wind on rings. *Journal of Physical Oceanography*, *17*(10), 1653–1667.
Ducet, N., Le Traon, P.-Y., & Reverdin, G. (2000). Global high-resolution mapping of ocean circulation from TOPEX/Poseidon and ERS-1 and-2. *Journal of Geophysical Research*, *105*(C8), 19,477–19,498.
Duhaut, T. H., & Straub, D. N. (2006). Wind stress dependence on ocean surface velocity: Implications for mechanical energy input to ocean circulation. *Journal of Physical Oceanography*, *36*(2), 202–211.
Eden, C., & Dietze, H. (2009). Effects of mesoscale eddy/wind interactions on biological new production and eddy kinetic energy. *Journal of Geophysical Research*, *114*, C05023. https://doi.org/10.1029/2008JC005129
Fairall, C., Bradley, E. F., Hare, J., Grachev, A., & Edson, J. (2003). Bulk parameterization of air-sea fluxes: Updates and verification for the COARE algorithm. *Journal of Climate*, *16*(4), 571–591.
Gula, J., Molemaker, M. J., & McWilliams, J. C. (2015). Gulf Stream dynamics along the southeastern US seaboard. *Journal of Physical Oceanography*, *45*(3), 690–715.
Gula, J., Molemaker, M. J., & McWilliams, J. C. (2016). Topographic generation of submesoscale centrifugal instability and energy dissipation. *Nature Communications*, *7*, 12811.
LaCasce, J. (2012). Surface quasigeostrophic solutions and baroclinic modes with exponential stratification. *Journal of Physical Oceanography*, *42*(4), 569–580.
Large, W. G., McWilliams, J. C., & Doney, S. C. (1994). Oceanic vertical mixing: A review and a model with a nonlocal boundary layer parameterization. *Reviews of Geophysics*, *32*(4), 363–404.
Le Traon, P., Nadal, F., & Ducet, N. (1998). An improved mapping method of multisatellite altimeter data. *Journal of Atmospheric and Oceanic Technology*, *15*(2), 522–534.
Lemarié, F., Kurian, J., Shchepetkin, A. F., Molemaker, M. J., Colas, F., & McWilliams, J. C. (2012). Are there inescapable issues prohibiting the use of terrain-following coordinates in climate models? *Ocean Modelling*, *42*, 57–79.
Lemarié, F., Samson, G., Redelsperger, J.-L., Madec, G., & Giordani, H. (2017). Toward an improved representation of air-sea interactions in high-resolution global oceanic forecasting systems, *2017 - Copernicus Marine week*. Brussels, Belgium: Copernicus.
Loveday, B. R., Durgadoo, J. V., Reason, C. J., Biastoch, A., & Penven, P. (2014). Decoupling of the Agulhas leakage from the Agulhas Current. *Journal of Physical Oceanography*, *44*(7), 1776–1797.
Luo, J.-J., Masson, S., Roeckner, E., Madec, G., & Yamagata, T. (2005). Reducing climatology bias in an ocean-atmosphere CGCM with improved coupling physics. *Journal of Climate*, *18*(13), 2344–2360.
Ma, X., Jing, Z., Chang, P., Liu, X., Montuoro, R., Small, R. J., et al. (2016). Western boundary currents regulated by interaction between ocean eddies and the atmosphere. *Nature*, *535*(7613), 533–537.
Marchesiello, P., Capet, X., Menkes, C., & Kennan, S. C. (2011). Submesoscale dynamics in tropical instability waves. *Ocean Modelling*, *39*(1), 31–46.
Marchesiello, P., Debreu, L., & Couvelard, X. (2009). Spurious diapycnal mixing in terrain-following coordinate models: The problem and a solution. *Ocean Modelling*, *46*, 156–169.
Marchesiello, P., McWilliams, J. C., & Shchepetkin, A. (2001). Open boundary conditions for long-term integration of regional oceanic models. *Ocean Modelling*, *3*(1), 1–20.
McClean, J. L., Bader, D. C., Bryan, F. O., Maltrud, M. E., Dennis, J. M., Mirin, A. A., et al. (2011). A prototype two-decade fully-coupled fine-resolution CCSM simulation. *Ocean Modelling*, *39*(1), 10–30.
McGillicuddy, D. J., Anderson, L. A., Bates, N. R., Bibby, T., Buesseler, K. O., Carlson, C. A., et al. (2007). Eddy/wind interactions stimulate extraordinary mid-ocean plankton blooms. *Science*, *316*(5827), 1021–1026.
McWilliams, J. C. (2008). The nature and consequences of oceanic eddies. *Ocean Modeling in an Eddying Regime*, *177*, 5–15.
Minobe, S., Kuwano-Yoshida, A., Komori, N., Xie, S.-P., & Small, R. J. (2008). Influence of the Gulf Stream on the troposphere. *Nature*, *452*(7184), 206–209.
Molemaker, M. J., McWilliams, J. C. M., & Capet, X. (2010). Balanced and unbalanced routes to dissipation in an equilibrated Eady flow. *Journal of Fluid Mechanics*, *654*, 35–63.
Oerder, V., Colas, F., Echevin, V., Masson, S., & Lemarié, F. (2018). Impacts of the mesoscale ocean-atmosphere coupling on the Peru-Chile ocean dynamics: The current-induced wind stress modulation. *Journal of Geophysical Research: Oceans*, *123*, 812–833. https://doi.org/10.1002/2017JC013294
Özgökmen, T. M., & Chassignet, E. P. (2002). Dynamics of two-dimensional turbulent bottom gravity currents. *Journal of Physical Oceanography*, *32*(5), 1460–1478.
Pacanowski, R. (1987). Effect of equatorial currents on surface stress. *Journal of Physical Oceanography*, *17*(6), 833–838.
Renault, L., McWilliams, J. C., & Gula, J. (2018). Dampening of submesoscale currents by air-sea stress coupling in the Californian Upwelling System. *Scientific Reports*, *8*(1), 13388.
Renault, L., McWilliams, J. C., & Masson, S. (2017). Satellite observations of imprint of oceanic current on wind stress by air-sea coupling. *Scientific Reports*, *7*(1), 17747.
Renault, L., McWilliams, J. C., & Penven, P. (2017). Modulation of the Agulhas Current retroflection and leakage by oceanic current interaction with the atmosphere in coupled simulations. *Journal of Physical Oceanography*, *47*(8), 2077–2100.

Renault, L., Molemaker, M. J., Gula, J., Masson, S., & McWilliams, J. C. (2016). Control and stabilization of the Gulf Stream by oceanic current interaction with the atmosphere. *Journal of Physical Oceanography*, *46*(11), 3439–3453.

Renault, L., Molemaker, M. J., Mcwilliams, J. C., Shchepetkin, A. F., Lemarié, F., Chelton, D., et al. (2016). Modulation of wind work by oceanic current interaction with the atmosphere. *Journal of Physical Oceanography*, *46*(6), 1685–1704.

Rio, M.-H., Mulet, S., & Picot, N. (2014). Beyond GOCE for the ocean circulation estimate: Synergetic use of altimetry, gravimetry, and in situ data provides new insight into geostrophic and Ekman currents. *Geophysical Research Letters*, *41*, 8918–8925. https://doi.org/10.1002/2014GL061773

Saha, S., Moorthi, S., Pan, H.-L., Wu, X., Wang, J., Nadiga, S., et al. (2010). The NCEP Climate Forecast System Reanalysis. *Bulletin of the American Meteorological Society*, *91*(8), 1015–1057.

Schoonover, J., Dewar, W., Wienders, N., Gula, J., McWilliams, J. C., Molemaker, M. J., et al. (2016). North Atlantic barotropic vorticity balances in numerical models*. *Journal of Physical Oceanography*, *46*(1), 289–303.

Scott, R. B., & Xu, Y. (2009). An update on the wind power input to the surface geostrophic flow of the World Ocean. *Deep Sea Research Part I: Oceanographic Research Papers*, *56*(3), 295–304.

Seo, H. (2017). Distinct influence of air–sea interactions mediated by mesoscale sea surface temperature and surface current in the Arabian Sea. *Journal of Climate*, *30*(20), 8061–8080.

Seo, H., Miller, A. J., & Norris, J. R. (2015). Eddy-wind interaction in the California Current System: Dynamics and impacts. *Journal of Physical Oceanography*, *46*(2015), 439–459.

Shchepetkin, A. F., & McWilliams, J. C. (2005). The Regional Oceanic Modeling System (ROMS): A split-explicit, free-surface, topography-following-coordinate oceanic model. *Ocean Modelling*, *9*(4), 347–404.

Skamarock, W., Klemp, J., Dudhia, J., Gill, D., & Barker, D. (2008). A description of the Advanced Research WRF version 3 (*Tech. rep.*) Boulder: NCAR. Note NCAR/TN-4751STR.

Soufflet, Y., Marchesiello, P., Lemarié, F., Jouanno, J., Capet, X., Debreu, L., & Benshila, R. (2016). On effective resolution in ocean models. *Ocean Modelling*, *98*, 36–50. https://doi.org/10.1016/j.ocemod.2015.12.004

Spall, M. (1996). Dynamics of the Gulf Stream/Deep Western Boundary Current crossover. Part I: Entrainment and recirculation. *Journal of Physical Oceanography*, *26*, 2152–2168.

Valcke, S. (2013). The OASIS3 coupler: A European climate modelling community software. *Geoscientific Model Development*, *6*(2), 373–388.

Xu, Y., & Scott, R. B. (2008). Subtleties in forcing eddy resolving ocean models with satellite wind data. *Ocean Modelling*, *20*(3), 240–251.